Adv. Radio Sci., 11, 313–318, 2013
www.adv-radio-sci.net/11/313/2013/
doi:10.5194/ars-11-313-2013
© Author(s) 2013. CC Attribution 3.0 License.

Advances in Radio Science

Enhanced sporadic *E* occurrence rates during the Geminid meteor showers 2006–2010

C. Jacobi[1], **C. Arras**[2], **and J. Wickert**[2]

[1]Institute for Meteorology, University of Leipzig, Stephanstr. 3, 04103 Leipzig, Germany
[2]German Research Centre for Geosciences GFZ, Potsdam, Department Geodesy & Remote Sensing, Telegrafenberg, 14473 Potsdam, Germany

Correspondence to: C. Jacobi (jacobi@uni-leipzig.de)

Abstract. Northern Hemisphere midlatitude sporadic *E* (E_s) layer occurrence rates derived from FORMOSAT-3/COSMIC GPS radio occultation (RO) measurements during the Geminid meteor showers 2006–2010 are compared with meteor rates obtained with the Collm (51.3° N, 13.0° E) VHF meteor radar. In most years, E_s rates increase after the shower, with a short delay of few days. This indicates a possible link between meteor influx and the production of metallic ions that may form E_s. There is an indication that the increase propagates downward, probably partly caused by tidal wind shear. However, the correlation between E_s rates and meteor flux varies from year to year. A strong correlation is found especially in 2009, while in 2010 E_s rates even decrease during the shower. This indicates that additional processes significantly influence E_s occurrence also during meteor showers. A possible effect of the semidiurnal tide is found. During years with weaker tidal wind shear, the correlation between E_s and meteor rates is even weaker.

1 Introduction

Sporadic *E* (E_s) layers are thin vertical regions of enhanced electron density in the lower ionosphere. Their origin is generally accepted to be vertical ion drift convergence driven by vertical shears in the horizontal tidal winds, with the long-living ions needed for the layers to be provided by meteors (Whitehead, 1960). There have been long discussions about how sporadic *E* layers are linked to meteor rates. The similarity of the seasonal cycles of both meteor rates and E_s occurrence rates or strength suggested a cause-and-effect explanation for the sporadic *E* layer seasonal dependence (Haldoupis et al., 2008).

However, not all features of the seasonal E_s cycle can be found in meteor rates, too. One reason may be that meteor radars, which are usually utilised to provide meteor rate seasonal cycles, only detect part of the incoming meteor flux. Another possible reason is that metallic ions are relatively long-lived and some details of short-term variability are thus not visible in E_s. Nevertheless, it is of interest whether short-period meteor events, especially meteor showers, may influence E_s rates.

The Geminids are a major meteor shower, which forms every year between December 4–17 with its peak activity on December 13 (at solar longitude $\lambda = 262°$). Its parent body is the asteroid 3200 Phaeton. Geminid shower meteors are relatively slow with a geocentric velocity of about 35 km/s (e.g., Stober et al., 2011a). Consequently, they burn at comparatively low altitudes and are thus well visible in the altitude range accessible to standard meteor radars (about 80–100 km). The Geminid meteor shower is the major shower visible in radio detections, while other showers are less well visible at least if the analysis is not focused on altitudes above about 100 km.

In this paper we present E_s occurrence rates detected by the GPS (Global Positioning System) radio occultation method using F3C (FORMOSAT-3/COSMIC, FORMOsa SATellite mission-3/Constellation Observing System for Meteorology, Ionosphere and Climate) data during the Geminid meteor showers 2006–2010, and compare these with meteor rates observed with VHF meteor radar. In Sects. 2 and 3 the methods are briefly introduced. In Sect. 4, we present time series of E_s and meteor count rates, which are discussed in Sect. 5. Section 6 concludes the paper.

2 Sporadic E analysis using FORMOSAT-3/COSMIC radio occultations

The F3C constellation was launched on 14 April 2006 and consists of six satellites (Anthes et al., 2008). The main scientific instrument aboard each satellite is a GPS receiver, which applies the GPS radio occultation technique (e.g., Kursinski et al., 1997) for vertical atmosphere sounding on a global scale.

To obtain information on the E_s occurrence we use signal-to-noise ratio (SNR) profiles of the 50 Hz GPS L1 signal below 120–140 km according to Arras et al. (2008). Strong changes in the vertical electron density gradients, as it is usual in presence of a sporadic E layer, appear as strong fluctuations in the SNR above about 85 km altitude. These disturbances are caused by signal divergence/convergence which leads to a decrease/increase of the signal intensity at the receiving antenna. The fluctuations are extracted from the background by applying a band pass filter which only accepts disturbances covering altitude intervals between 1.0 and 12.5 km. If the standard deviation of the SNR in a 2.5 km interval exceeds the threshold of 0.2, the disturbance in the SNR profile is regarded as significant. Since E_s are very thin layers, the standard deviation should rise abruptly. Consequently, a second criterion is introduced defining that the standard deviation has to rise suddenly by more than 0.14 between two adjacent intervals. In order to avoid using disturbances resulting from other effects than sporadic E, all profiles are excluded from further investigation, if the standard deviation exceeds the threshold of 0.2 in more than five intervals. The maximum deviation from the mean profile represents the approximate altitude of the sporadic E layer (e.g., Arras et al., 2008, 2009). Note that this method does not provide information about the strength of the E_s layer (amplitude of related electron density) but only on the occurrence rates in a given time and space interval.

GPS RO data are not uniformly distributed around the globe (see also Arras et al., 2009). In the left panel of Fig. 1, the total number of occultations per 5 degree latitude interval between 4 and 17 December, taken as the average of the years 2006–2010, are presented as black line. In the lower part of the panel, the occurrence rates, defined as the number of detected E_s divided by the number of occultations in a 5 km height and 5 degrees latitude gate, are presented. The majority of E_s is found in the summer hemisphere, but there is also considerable E_s activity at lower winter latitudes. The maximum number of E_s is found at altitudes slightly above 100 km. There is a tendency for lower altitudes in the winter hemisphere. In the right panel of Fig. 1, the 20–60° N mean occurrence rates per 1 km height interval are presented. Most E_s are found between 90 and 110 km. Note, however, that this result is partly due to the upper limit of the GPS RO profiles, which is set to around 120 km for F3C.

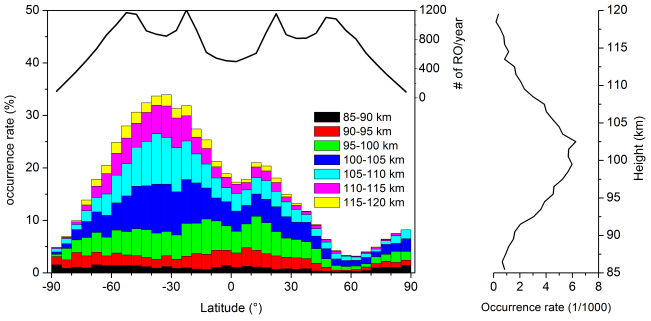

Fig. 1. Left panel: 2006–2010 mean sporadic E occurrence rates per 5 km height interval for different 5° latitude bands for the time interval 4–17 December of each year. Right panel: Mean occurrence rates per 1 km height interval for all latitudes between 20° N and 60° N and for the same time interval.

3 Collm meteor radar measurements

At Collm, Germany (51.3° N, 13.0° E), a SKiYMET all sky meteor radar is operated at 36.2 MHz since summer 2004. The antenna system consists of one 3-element Yagi transmitting antenna and five 2-element Yagi receiving antennas, forming an interferometer. Peak power is 6 kW. Pulse repetition frequency is 2144 Hz, but effectively only 536 Hz, due to 4-point coherent integration. The sampling resolution is 1.87 ms. The angular and range resolutions are ∼2° and 2 km, respectively. The pulse width is 13 µs, the receiver bandwidth is 50 kHz (see also Stober et al., 2011b).

We consider zenith angles between 0° and 70°, and distances of up to 400 km from the transmitter. Meteor count rates are taken every 2 h, and running 24 h means are calculated. In the following, we consider the Geminid meteor shower as one that is visible in each altitude interval, and which considerably influences meteor count rates. We analyse count rates at altitudes between 75 and 105 km. The radar is also used for wind measurements, using Doppler frequency shift of the reflected radio wave from meteor trails and minimising the squared difference between radial winds and the half-hourly horizontal winds projected on these. Mean winds and tidal parameters are calculated using least-squares fitting (e.g., Jacobi, 2011).

4 Results

As an example, in Fig. 2 the 24 h mean meteor count rates and E_s occurrence rates are shown for the year 2010. After the minimum in late winter/early spring there is an increase and maximum E_s and meteor rates in summer. This behaviour has led to the conclusion that the annual cycle of meteor rates is responsible for the seasonal cycle of E_s (Haldoupis et al., 2008). After midsummer however, the meteor rates remain fairly high until about November while E_s

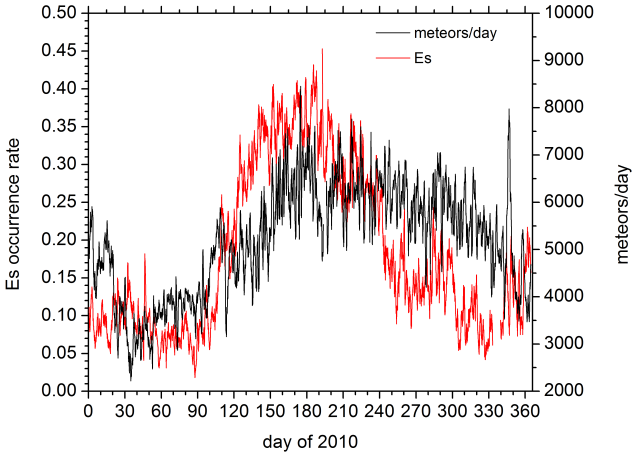

Fig. 2. 24 h mean Collm meteor count rates and 20–60° N mean sporadic E occurrence rates in 2010.

occurrences decrease. In December there is usually an increase in E_s occurrence, which is not present in all years.

Figure 2 shows that the seasonal cycle of meteor rates only partly explains the seasonal cycle of E_s. On shorter time scales, however, some peculiarities are found when E_s and meteor rates behave similarly. One of them is the maximum of E_s rates during the Geminid meteor showers in December. This may indicate that strong meteor showers could lead to enhanced E_s rates owing the increasing mass flux and thus ion production rate.

Two examples of E_s and meteor rates during the Geminid meteor showers in different years are presented in Fig. 3. We added the 2-hourly mean meteor rates multiplied by 12, to give an impression how the 24 h means are obtained. Meteor rates have a distinct diurnal cycle with maximum rates in the early morning. This may influence the trends of the 24 h means presented and definitely makes it difficult to detect the exact time of a meteor shower peak. The E_s rates are taken over all longitudes and thus do not show the diurnal cycle. In 2006, the E_s rates increase with some delay after the time of increasing meteor rates. Meteor rates after solar longitude $\lambda = 256°$ show a double-peak structure, which is also represented in E_s rates. In 2010, however, the picture is not that clear. E_s rates undergo an oscillation not very clearly linked to the Geminid shower. However, in most years an E_s increase is preceded by an increase in meteor rates with a time delay of 2 to 3 days, although there is no quantitative connection between the respective maxima.

On the left panel of Fig. 4, 5 yr averages of E_s occurrence and meteor rates are presented together with the standard error. Owing to the small number of years included, the error is partly large due to interannual variability. One can see that on average, E_s rates maximise about 2.5 days after the meteor rates. Note that there is an E_s maximum also shortly before the meteor rate maximum, however, this is preceded by a weak enhancement of meteor rates, too. In the right panel of Fig. 4, the cross-correlation functions, taken from data of the days #335–355 of each year, are presented. One can see that the E_s-meteor rate correlation in respective years behave in different manners, but there is a tendency for the cross-correlation to maximise at a lag of few days, except for 2007, when the correlation is low at a lag of few days.

5 Discussion

Considering the standard error bars of the 5 year mean E_s rates, it can be concluded that the enhancement of E_s after the Geminid meteor shower is hardly significant. In part this can be due to the small number of years considered, but definitely there is considerable interannual variability of the E_s behaviour. As is the case in 2007, during some years E_s does not seem to be strongly influenced by the meteor shower, while in other years a rather strong correlation is found. Clearly, other influencing factors must play a role.

The wind shear theory predicts that at midlatitudes E_s are formed at the convergence nodes of vertical ion drift owing mainly to vertical shear of the zonal wind. Comprehensive overviews on this effect has been presented, e.g., by Haldoupis (2011, 2012). Generally, E_s layers form at altitudes of 120–130 km, which is at the upper limit or slightly above the region covered by the used RO. The main contribution to wind shear is by the semidiurnal tide (SDT), such that the SDT signature is clearly visible in E_s phases (e.g. Arras, 2009). Figure 5 presents SDT zonal wind amplitudes as measured at Collm during December 2006–2010. One can see that the amplitudes are smaller in 2007, 2008, and 2010 compared to 2006 and 2009. Comparing this with Fig. 4 reveals that these are the years when the cross-correlation function at lag up to about 5 days does not exceed values of 0.5, while in 2006 and 2009 larger values are found. Although the number of years considered is too small to draw more substantial conclusions, and the SDT amplitudes are only a proxy for the wind shear, this nevertheless indicates that SDT wind shear variability may modulate the E_s reaction on meteor showers.

It has to be noted that possible enhancement of E_s after meteor showers should be a rather indirect process. To date there is no proof that after the Geminid shower the concentration of metallic ions is really enhanced, and measurements showed inconclusive and partly contradicting results. For example, Dunker et al. (2013) found a decrease in sodium column abundance during the 2010 Geminid meteor shower, which is consistent with the decrease in E_s rates shown in the right panel of Fig. 3. One reason may be that the mass influx of the Geminids is small compared with the sporadic background (e.g. Ceplecha et al., 1998). The Collm radar is not sensitive to meteors above about 105 km, and the meteor rates provided here are therefore qualitative when they are used to describe the total meteor flux. Haldoupis et al. (2008) also pointed out that they only found a poor

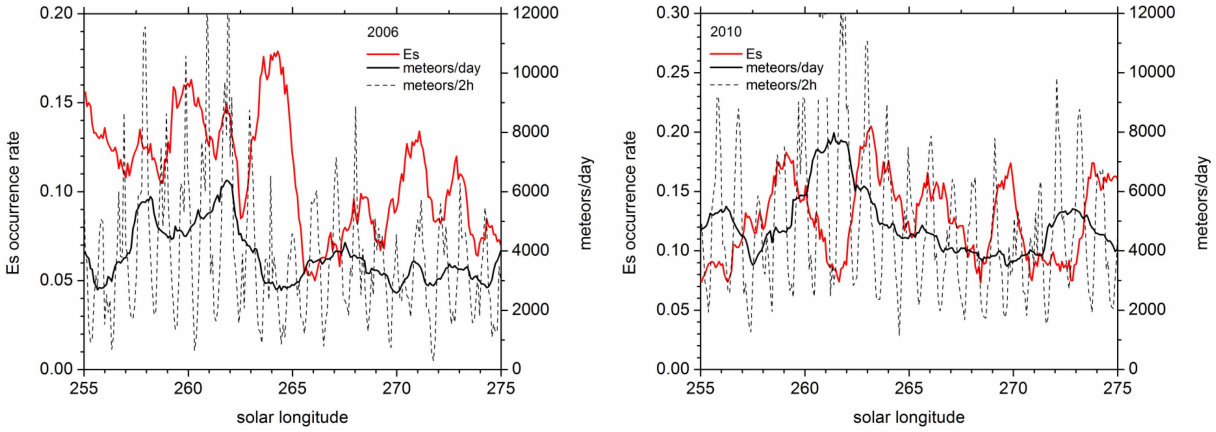

Fig. 3. Daily sporadic E layer occurrence rates in 2006 (left) and 2010 (right). Daily mean meteor rates are added, as well as 2-hourly meteor rates multiplied by 12.

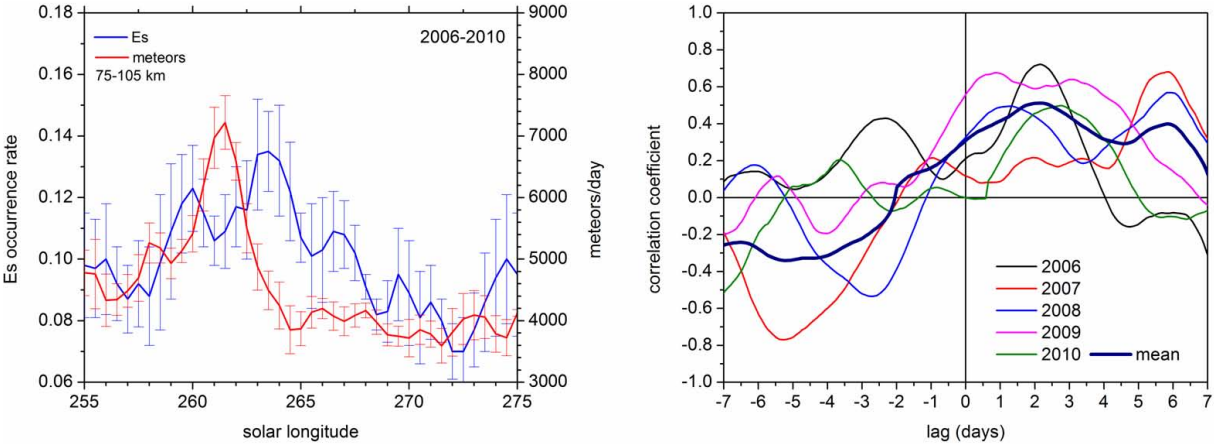

Fig. 4. Left panel: 2006–2010 mean sporadic E occurrence rates (blue) and 24 h mean meteor count rates (red). Standard errors are added. Right panel: cross-correlation functions between sporadic E occurrence rates and meteor count rates. Positive lag denotes meteor rate changes heading E_s ones.

correlation between the Geminid meteor rates and E_s critical frequencies. Moreover, other slow meteor showers like the Quadrantids in January do not seem to have considerable influence on the E_s rates (see Fig. 2).

Another open question refers to the time delay between meteor shower and E_s increase. To shed more light on this, we present in Fig. 6 cross-correlation functions between E_s occurrence rates and meteor count rates in 2009 at different altitudes. The curves are shifted by 0.2 against each other to visualize the height dependence. One can clearly see that there is a vertical shift of the delay of E_s rates with respect to the meteor rates, so that at lower altitudes the E_s rates increase later. This means that, although the Geminid meteors are found in every height accessible to the Collm radar, ions probably first form at larger altitudes and are then transported downwards. In total, this leads to a time delay of the overall E_s occurrence rates. However, the descent speed of E_s layers in winter is usually of the order of 2 km h^{-1} at altitudes above

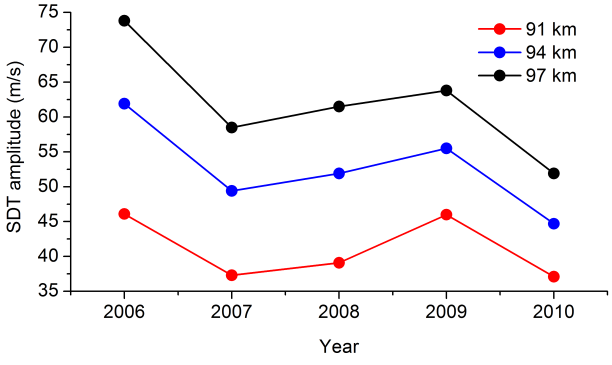

Fig. 5. December mean semidiurnal tidal zonal wind amplitudes over Collm.

about 100 km (Arras et al., 2009), so that there is another reason for delay of the layer formation. Generally, the E_s layer

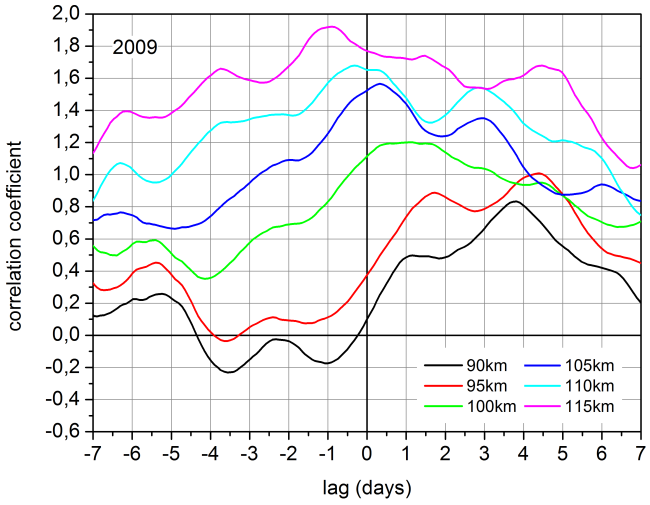

Fig. 6. Cross-correlation functions between sporadic E occurrence rates and meteor count rates in 2009 for different 10 km E_S height gates centered at the heights given in the legend. Positive lag denotes meteor rate changes heading E_S ones. The curves are shifted by 0.2 against each other to visualize the height dependence.

descent follows the phase speed of the SDT convergent node at altitudes well above about 100 km, but slows down owing to enhanced ion-neutral collisions and also since the diurnal tide with a shorter wavelength provides the downward transport (Haldoupis, 2012; Haldoupis et al., 2006; Christakis et al., 2009). Indeed, Arras et al. (2009, their Fig. 6) have found a delay of E_S phase downward progression with respect to SDT wind shear ones, but these gave rise to only few hours delay and would not explain a delay of more than one day. Other mechanisms, like a possible mean downward wind, could be the reason for the longer delay in some cases.

6 Conclusions

Our results indicate that there is a tendency for sporadic E layer occurrence rates to increase after the Geminid meteor shower. This increase is observed with an average time delay of 2.5 days. This effect is variably strong pronounced in different years, in particular during 2007 it appeared to be quite weak. Comparison with SDT amplitudes indicates a possible relationship with changing wind shear magnitudes.

Taking into account the small number of years considered so far and the comparatively large error bars of the mean effect, conclusions should be drawn with care. This is also the case, since supporting evidence of increasing metal concentration after meteor showers is not available. Further experimental and modelling studies are required to substantiate the results. For example, ionosonde measurements will be helpful to increase the upper boundary of the observational data base and will shed more light on the layer formation and downward propagation effect.

Acknowledgements. This study was partly supported by Deutsche Forschungsgemeinschaft under JA 836/22-1. We acknowledge UCAR (Boulder, US) and NSPO (Taiwan) for the provision of FORMOSAT-3/COSMIC data and related support. Solar longitudes have been calculated based on those provided by the International Meteor Organisation (IMO) on http://www.imo.net/data/solar.

References

Anthes, R. A., Bernhardt, P. A., Chen, Y., Cucurull, L., Dymond, K., F., Ector, D., Healy, S. B., Ho, S.-P., Hunt, D. C., Kuo, Y.-H., Liu, H., Manning, K., McCormick, C., Meehan, T. K., Randel, W. J., Rocken, C., Schreiner, W. S., Sokolovskiy, S. V., Syndergaard, S., Thompson, D. C., Trenberth, K. E., Wee, T.-K., Yen, N. L., and Zeng, Z.: The COSMIC/FORMOSAT-3 Mission: Early Results, B. Am. Meteorol. Soc., 83, 313–333, doi:10.1175/BAMS-89-3-313, 2008.

Arras, C., Wickert, J., Beyerle, G., Heise, S., Schmidt, T., and Jacobi, Ch.: A global climatology of ionospheric irregularities derived from GPS radio occultation, Geophys. Res. Lett., 35, L14809, doi:10.1029/2008GL034158, 2008.

Arras, C., Jacobi, Ch., and Wickert, J.: Semidiurnal tidal signature in sporadic E occurrence rates derived from GPS radio occultation measurements at midlatitudes. Ann. Geophys., 27, 2555–2563, doi:10.5194/angeo-27-2555-2009, 2009.

Ceplecha, Z., Borovicka, J., Elford, W. G., Revelle, D. O., Hawkes, R. L., Porubcan, V., and Simek, M.: Meteor phenomena and bodies, Space Sci. Rev., 84, 327–471, 1998.

Christakis, N., Haldoupis, C., Zhou, Q., and Meek, C.: Seasonal variability and descent of mid-latitude sporadic E layers at Arecibo, Ann. Geophys., 27, 923–931, doi:10.5194/angeo-27-923-2009, 2009.

Dunker, T., Hoppe, U.-P., Stober, G., and Rapp, M.: Development of the mesospheric Na layer at 69° N during the Geminids meteor shower 2010, Ann. Geophys., 31, 61–73, 2013, http://www.ann-geophys.net/31/61/2013/.

Haldoupis, C.: A tutorial review on sporadic E layers, in Aeronomy of the Earth's Atmosphere and Ionosphere. IAGA Special Sopron Book Series 2, 381–394, doi:10.1007/978-94-007-0326-1-29, 2011.

Haldoupis, C.: Midlatitude sporadic E. A typical paradigm of atmosphere-ionosphere coupling, Space Sci. Rev., 168, 441–461, doi:10.1007/s11214-011-9786-8, 2012.

Haldoupis, C., Meek, C., Christakis, N., Pancheva, D., and Bourdillon, A.: Ionogram height-time-intensity observations of descending sporadic E layers at mid-latitudes, J. Atmos. Solar Terr. Phys., 68, 539–557, doi:10.1016/j.jastp.2005.03.020, 2006.

Haldoupis, C., Pancheva, D., Singer, W., Meek, C., and MacDougall, J.: An explanation for the seasonal dependence of midlatitude sporadic E layers, J. Geophys. Res., 112, A06315, doi:10.1029/2007JA012322, 2008.

Jacobi, Ch.: Meteor radar measurements of mean winds and tides over Collm (51.3° N, 13° E) and comparison with LF drift measurements 2005–2007, Adv. Radio Sci., 9, 335–341, doi:10.5194/ars-9-335-2011, 2011.

Kursinski, E. R., Hajj, G. A., Schofield, J. T., Linfield, R. P., and Hardy, K. R.: Observing earth's atmosphere with radio occultation measurements using the global positioning system, J. Geophys. Res., 102, 23429–23465, 1997.

Stober, G., Jacobi, Ch., and Singer, W.: Meteoroid mass determination from underdense trails. J. Atmos. Solar-Terr. Phys., 73, 895–900, doi:10.1016/j.jastp.2010.06.009, 2011a.

Stober, G., Singer, W., and Jacobi, Ch.: Cosmic radio noise observations using a mid-latitude meteor radar, J. Atmos. Solar-Terr. Phys., 73, 1069–1076, doi:10.1016/j.jastp.2010.07.018, 2011b.

Whitehead, J. D.: Formation of the sporadic E layer in the temperate zones, Nature, 188, 567–567, 1960.